

Adaptive Signal Detection in Auto-Regressive Interference with Gaussian Spectrum

M. R. Moniri*, M. M. Nayebi** and A. Sheikhi***

Abstract: A detector for the case of a radar target with known Doppler and unknown complex amplitude in complex Gaussian noise with unknown parameters has been derived. The detector assumes that the noise is an Auto-Regressive (AR) process with Gaussian autocorrelation function which is a suitable model for ground clutter in most scenarios involving airborne radars. The detector estimates the unknown parameters by Maximum Likelihood (ML) estimation for the use in the Generalized Likelihood Ratio Test (GLRT). By computer simulations, it has been shown that for large data records, this detector is Constant False Alarm Rate (CFAR) with respect to AR model driving noise variance. Also, measurements show the detector excellent performance in a practical setting. The detector's performance in various simulated and actual conditions and the result of comparison with Kelly's GLR and AR-GLR detectors are also presented.

Keywords: CFAR, GLR Test, Radar Detection.

1 Introduction

In a non-stationary and/or non-homogeneous interference environment of unknown statistics, adaptive detection algorithms, such as Sample Matrix Inversion (SMI) [1] and Kelly's Generalized Likelihood Ratio (GLR) algorithms [2], can suffer severe detection performance degradation, simply owing to the lack of sufficient amount of independent and identically distributed (iid) data from which the system can learn (estimate) the statistics of the environment. In [3-5] multiband SMI and GLR algorithms are proposed and have been shown to deliver a significantly improved detection performance as compared with corresponding single-band algorithms. These multiband algorithms are quite general in the sense that they do not assume that the interference covariance matrix has any special structure in addition to the Hermitian. To further improve the detection performance, one may exploit the structural information of the interference covariance. In

many situations of practical interest, interference data process can be modeled by an Auto-Regressive (AR) process. Sheikhi [6] and Kay [7-8] have exploited AR modeling for the interference in their GLR algorithms.

Sheikhi named his detector AR-GLR. Also, in [9] and [16] the extended AR-GLR for a multichannel application has been presented by Moniri. But if one can model the interference in a more precise way, it is expected to have a detector with a better performance based on this model.

So, this work is motivated by a desire to detect the radar target of unknown amplitude and known Doppler in additive AR noise, with Gaussian correlation matrix, based on GLR test. As it will be shown by computer simulations, our detector has better performance as compared with Kelly's GLR and AR-GLR detectors. In Section 2, we introduce notations and discuss the interference model. The detection problem is defined and the likelihood ratio is developed in Section 3. Simulation results and the detector performance against measured data are presented in Section 4. And finally, the conclusions are given at the end of the paper.

2 Preliminaries

In this section, we introduce notations and terminologies which are utilized throughout this work.

Consider the discrete complex process $y(k)$ received by a single-sensor pulsed radar system in which the detection problem is given by:

Iranian Journal of Electrical & Electronic Engineering, 2008.

Paper first received 14th April 2007 and in revised form 14th January 2008.

* The Author is with the Department of Engineering, Shahr_e_Rey Islamic Azad University, Tehran, Iran.

E-mail: mr_moniri_h@yahoo.com.

** The Author is with the Department of Electrical Engineering, Sharif University of Technology, Tehran, Iran.

E-mail: nayebi@sharif.edu.

*** The Author is with the Department of Engineering, Shiraz University, Shiraz, Iran.

E-mail: sheikhi@succ.shirazu.ac.ir.

$$\begin{aligned}
H_0 : \underline{y}(0) &= \underline{n}(0) \\
\underline{y}(k) &= \underline{n}(k) \quad (k=1,2,\dots,K) \\
H_1 : \underline{y}(0) &= \underline{n}(0) + \alpha \underline{S} \\
\underline{y}(k) &= \underline{n}(k) \quad (k=1,2,\dots,K)
\end{aligned} \tag{1}$$

where $\underline{y}(k)$ is a complex N -dimensional vector (corresponding to N -pulse train). $\underline{y}(0)$ denotes the primary data and for $k = 1, 2, \dots, K$ they are secondary data which are iid and include no targets. \underline{S} is also a complex N -dimensional vector which denotes the target signal and is given by:

$$\underline{S} = [s_1 \ s_2 \ \dots \ s_N]^T = [1 \ e^{j\Omega} \ \dots \ e^{j(N-1)\Omega}]^T \tag{2}$$

where T stands for the transpose. this vector corresponds to a target whose Doppler is Ω , which is assumed to be known. α is an unknown complex amplitude of the reflected signal from the target. $\underline{n}(k)$ is also a complex N -dimensional vector denoting the clutter

$$\underline{n}(k) = [n_{k,1} \ n_{k,2} \ \dots \ n_{k,N}]^T \tag{3}$$

which is assumed to be an $AR(M, \underline{a}, \sigma_u^2)$, AR process of order M and parameters \underline{a} and σ_u^2 , given by:

$$n_{k,i} = \sum_{j=1}^M a_j n_{k,i-j} + u_i \tag{4}$$

where u_i is zero-mean discrete complex white Gaussian noise with variance σ_u^2 , and $\underline{a} = [a_1 a_2 \dots a_M]^T$ is the AR parameter vector (the AR model is proposed specially for characterization of ground clutter, as in an airborne system, which is our primary interest). We assume that \underline{a} and σ_u^2 are also unknown but \underline{a} can be expressed in terms of other unknown parameters which are derived from correlation function shape.

In this work, at first we fix the form of the correlation function and then apply the GLR theory on unknown parameters. We consider the correlation function $R(1)$ which is defined as

$$R(1) = E \left[\begin{matrix} n_{k,n} & n_{k,1-n}^* \end{matrix} \right] \begin{matrix} (k = 0, 1, \dots, K) \\ (n = 1, 2, \dots, N) \end{matrix} \tag{5}$$

This means a similar correlation function for interference in both primary and secondary data

samples. We now consider modeling $R(1)$ with functional forms that will enable us to obtain a variety of spectral distributions. We express this function in the form of:

$$R(1) = K_n f_n(\lambda, 1 - l_0) \exp(j\theta_n(1)) \tag{6}$$

The quantity λ is defined as a temporal correlation parameter, which provides a measure for the correlation between discrete samples of the process. The function $f_n(\bullet)$ is selected to specify the shape of the correlation function magnitude; l_0 is the lag value at which the corresponding real function $f_n(\bullet)$ has a peak value of unity. $\theta_n(\bullet)$ show the Doppler shifting caused by platform motion. In this paper, as Doppler shifting has been assumed to be known, we have let $\theta_n(\bullet) = 0$. For the temporal correlation functions $l_0 = 0$ and the constant K_n is a real, normalizing coefficient. In [10], the special cases of Gaussian, exponential and sinc shaped correlation function are considered. Here we use Gaussian form which will be shown in section 4 to be a suitable model for our measurements. So, we consider

$$f_n(\lambda, 1) = (\lambda)^2 \tag{7}$$

so that Eq. (6) becomes

$$R(1) = \sigma^2 (\lambda)^2 \tag{8}$$

where σ^2 is the variance of the zero mean process and λ is a real parameter such that $0 \leq \lambda \leq 1$.

Now, the Yule-Walker equation can be used to determine the AR coefficients of the process, as could be derived from (4)

$$\begin{bmatrix} R(0) & R(1) & \dots & R(M) \\ R(-1) & R(0) & \dots & R(M-1) \\ \vdots & \vdots & & \vdots \\ R(-M) & R(-M+1) & \dots & R(0) \end{bmatrix} \begin{bmatrix} 1 \\ a_1 \\ \vdots \\ a_M \end{bmatrix} = \begin{bmatrix} \sigma_u^2 \\ 0 \\ \vdots \\ 0 \end{bmatrix} \tag{9}$$

The AR power spectral density (psd) which would result from determined AR coefficients provides a fit to the desired spectrum. Alternatively, when these coefficients are used in (4), we are able to generate processes which provide a fit to the desired spectrum in a MMSE sense. In this work, however, we are concerned with parameter estimation. So Eqs. (8) and (9) give us \underline{a} and σ^2 in terms of λ and σ_u^2 and then we use $\underline{a}(\lambda) = [a_1(\lambda) \ a_2(\lambda) \ \dots \ a_M(\lambda)]^T$ instead of \underline{a} .

As an example, for a second order ($M = 2$) AR process $\underline{a}(\lambda)$ is given by:

$$\underline{a}(\lambda) = [-\lambda(\lambda^2 + 1) \quad \lambda^2]^T \quad (10)$$

and

$$\sigma^2 = \frac{\sigma_u^2}{1 - \lambda^2 - \lambda^4 + \lambda^6} \quad (11)$$

3 The Detection Problem

In this section, we discuss the detection problem addressed in this paper which is expressed as Eq. (1). We assume that α , λ and σ_u^2 are unknown but fixed constants which are the same under either hypothesis. The GLR theory can then be applied here. The resulting detector compares the generalized likelihood ratio, L_{GLR} , with a threshold η .

$$L_{\text{GLR}} = \frac{\max_{\sigma_u^2, \lambda, \alpha} f_Y(\underline{y}(0), \underline{y}(1), \dots, \underline{y}(K) | H_1, \sigma_u^2, \lambda, \alpha)}{\max_{\sigma_u^2, \lambda, \alpha} f_Y(\underline{y}(0), \underline{y}(1), \dots, \underline{y}(K) | H_0, \sigma_u^2, \lambda, \alpha = 0)} \quad (12)$$

$$= \frac{f_Y(\underline{y}(0), \underline{y}(1), \dots, \underline{y}(K) | H_1, \hat{\sigma}_u^2, \hat{\lambda}_1, \hat{\alpha})}{f_Y(\underline{y}(0), \underline{y}(1), \dots, \underline{y}(K) | H_0, \hat{\sigma}_u^2, \hat{\lambda}_0, \alpha = 0)} \Bigg\}_{H_1} \eta$$

where $f_Y(\underline{y}(0), \underline{y}(1), \dots, \underline{y}(K) | H_i, \sigma_u^2, \lambda_i, \alpha)$ is a conditional Probability Density Function (PDF) under hypothesis H_i , and λ_i , σ_u^2 and α are the maximum likelihood estimates of λ , σ_u^2 and α , respectively, under hypothesis H_i . Since $\underline{u}(k)$ is assumed to be Gaussian, the conditional PDF of $y(k)$ will be also Gaussian. It can be shown that for AR processes with poles not too close to the unit circle, we have [11]

$$f_1 = f_Y(\underline{y}(0), \underline{y}(1), \dots, \underline{y}(K) | H_1, \sigma_u^2, \lambda, \alpha)$$

$$\cong \left(\frac{1}{\pi^N \sigma_u^{2N}} \right)^{K+1} \prod_{k=0}^K \exp \left[-\frac{1}{\sigma_u^2} \sum_{n=M+1}^N \left| x_{k,n} - \sum_{j=1}^M a_j(\lambda) x_{k,n-j} \right|^2 \right] \quad (13)$$

where $x_{0,n} = y_{0,n} - \alpha s_n$ and $x_{k,n} = y_{k,n}$ for $k = 1, 2, \dots, K$, and for f_0 we have

$$f_0 = f_Y(\underline{y}(0), \underline{y}(1), \dots, \underline{y}(K) | H_0, \sigma_u^2, \lambda, \alpha = 0)$$

$$\cong \left(\frac{1}{\pi^N \sigma_u^{2N}} \right)^{K+1} \prod_{k=0}^K \exp \left[-\frac{1}{\sigma_u^2} \sum_{n=M+1}^N \left| y_{k,n} - \sum_{j=1}^M a_j(\lambda) y_{k,n-j} \right|^2 \right] \quad (14)$$

As shown in the Appendix, by using Eqs. (13) and (14) in Eq. (12), the detector is derived and given by:

$$\ln L_{\text{GLR}} = -N(K+1) \left(\ln(\hat{\sigma}_u^2) - \ln(\hat{\sigma}_u^2) \right) \Bigg\}_{H_1} \eta \quad (15)$$

where

$$\hat{\sigma}_u^2 = \frac{1}{N(K+1)} (\underline{u} - \underline{Y} \underline{a}(\hat{\lambda}_0))^H (\underline{u} - \underline{Y} \underline{a}(\hat{\lambda}_0)) \quad (16)$$

in which Y and u are defined as:

$$\underline{Y} = [\underline{Y}_0 \quad \underline{Y}_1 \quad \dots \quad \underline{Y}_K]^T, \underline{Y}_i = \begin{bmatrix} y_{i,M} & \dots & y_{i,1} \\ \vdots & \ddots & \vdots \\ y_{i,N-1} & \dots & y_{i,N-M} \end{bmatrix} \quad (17)$$

$$\underline{u} = [\underline{u}_0^T \quad \underline{u}_1^T \quad \dots \quad \underline{u}_K^T]^T, \underline{u}_i = [y_{i,M+1} \quad \dots \quad y_{i,N}]$$

and λ_0 is the root of Eq. (18) in the interval $[0 \quad 1]$:

$$\frac{d \underline{a}^H(\lambda)}{d\lambda} \underline{Y}^H \underline{Y} \underline{a}(\lambda) + \underline{a}^H(\lambda) \underline{Y}^H \underline{Y} \frac{d \underline{a}(\lambda)}{d\lambda} - \frac{d \underline{a}^H(\lambda)}{d\lambda} \underline{Y}^H \underline{u} - \underline{u}^H \underline{Y} \frac{d \underline{a}(\lambda)}{d\lambda} = 0 \quad (18)$$

which minimizes $\|\underline{u} - \underline{Y} \underline{a}(\lambda)\|^2$.

On the other hand

$$\hat{\sigma}_u^2 = \frac{1}{N(K+1)} (\underline{u}' - \underline{Y}' \underline{a}(\hat{\lambda}_1))^H (\underline{u}' - \underline{Y}' \underline{a}(\hat{\lambda}_1)) \quad (19)$$

in which \underline{Y}' and \underline{u}' are defined as

$$\underline{Y}' = [\underline{Y}'_0 \quad \underline{Y}'_1 \quad \dots \quad \underline{Y}'_K]^T, \underline{Y}'_i = \underline{H} \underline{Y}_i \quad (20)$$

$$\underline{u}' = [\underline{u}'_0^T \quad \underline{u}'_1^T \quad \dots \quad \underline{u}'_K^T]^T, \underline{u}'_i = \underline{H} \underline{u}_i$$

Y_i and u_i are defined in Eq. (17) and H is defined as

$$\underline{H} = \underline{I} - \frac{\underline{\phi} \underline{\phi}^H}{\underline{\phi}^H \underline{\phi}} \quad (21)$$

which is the projection matrix of the null space of $\underline{\phi}$ where

$$\underline{\phi} = [1 \quad e^{j\Omega} \quad \dots \quad e^{j(N-M-1)\Omega}] \quad (22)$$

and λ_1 is the root of Eq. (23) in the interval $[0 \ 1]$:

$$\begin{aligned} \frac{d\mathbf{a}^H(\lambda)}{d\lambda} \mathbf{Y}'^H \mathbf{Y}' \mathbf{a}(\lambda) + \mathbf{a}^H(\lambda) \mathbf{Y}'^H \mathbf{Y}' \frac{d\mathbf{a}(\lambda)}{d\lambda} \\ - \frac{d\mathbf{a}^H(\lambda)}{d\lambda} \mathbf{Y}'^H \mathbf{u}' - \mathbf{u}'^H \mathbf{Y}' \frac{d\mathbf{a}(\lambda)}{d\lambda} = 0 \end{aligned} \quad (23)$$

It is notable that in practical applications, an analytic solution for either Eq. (18) or (23) to obtain λ_0 or λ_1 can be very difficult. This can be resolved by using an approximate minimization of $|\underline{\mathbf{u}} - \mathbf{Y}\mathbf{a}(\lambda)|^2$ and $|\underline{\mathbf{u}} - \mathbf{Y}\mathbf{a}(\lambda)|^2$ in a grid search. Evidently, the performance of the system will be better when the step between pre assumed parameter values is less. The highest value of loss occurs when the actual temporal correlation parameter (λ) is in the middle of two pre-assumed values.

Since this detector assumes that $\underline{\mathbf{n}}(k)$ is an AR(M) process with Gaussian correlation function and the target has a Doppler of Ω , we call it Auto-Regressive, Gaussian correlation GLR (AR-GC-GLR(M, Ω)). The detector structure is shown in Fig. 1. An estimate of a pre-whitener is formed under both hypotheses, but under hypothesis H_1 the data are first projected on the null space of the vector ϕ . The power of the whitened time series is then estimated (using the covariance method in AR parameter estimation), transformed by a logarithmic operator and finally their difference is compared to a threshold.

It is also Notable that if the target model is generalized so that the target Doppler is assumed to be unknown, the likelihood ratio obtained in Eq. (15) must next be maximized over Ω . This maximization can not be carried out explicitly, but the standard technique is to approximate it by evaluating the test statistic for a discrete set of target Dopplers, forming a detector bank, and declaring target presence if any detector exceeds the threshold.

4 Detection Results Using Computer Simulations and Clutter Measurements

The performance of AR-GC-GLR detector for finite data length is evaluated through computer simulation. The case given by Eq. (1) is considered, where $\mathbf{n}(k)$ is an AR process of order M with parameters $\mathbf{a}(\lambda)$ and σ_u^2 . Similar [2, 7, 13], in these simulations signal to interference ratio (SINR) is defined as:

$$\text{SINR} = |\alpha|^2 \underline{\mathbf{S}}^H \mathbf{R}_N^{-1} \underline{\mathbf{S}} = |\alpha|^2 d \quad (24)$$

where \mathbf{R}_N is the actual correlation matrix of $\mathbf{n}(k)$ and computed using λ and σ_u^2 . In all of the simulations, the

order of process (M) is 2, $\sigma_u^2 = 2$ and $|\alpha|$ is adjusted to yield the given SINR. We used 10^5 samples in each simulation, So the curves are acceptable only for $P_{fa} > 10^{-3}$. Fig. 2 demonstrates probability of detection versus probability of false alarm for signal to interference ratios. As could be expected, for a given P_{fa} increasing SINR the performance of the detector (i.e. P_d) is improved.

Performance improvement by increasing the observation length is demonstrated in Fig. 3.

The dependence of the detection performance to secondary data is depicted in Fig. 4 where the performance is improved as more secondary data is used.

Fig. 5 shows the improvement of the detection performance by increasing the temporal correlation parameter (1) that is expected because of the chance of the detector to have a better estimation of the clutter behaviors when we have more correlation in our samples.

In fig. 6 the CFAR property of AR-GC-GLR with respect to s_u^2 for finite data lengths is investigated. In this simulation AR-GC-GLR (2,1) with $h = 4$ is used. $\mathbf{n}(0)$ is AR(2) process with $l=0.9$ and no secondary data is used. P_{fa} against s_u^2 is shown for $N = 20$, $N = 50$ and $N = 200$. In all three cases P_{fa} is approximately constant hence the detector is CFAR.

Fig. 7 demonstrates a comparison with Kelly's GLR and AR-GLR detectors. We can see high superiority of AR-GC-GLR. This superiority is the result of using a priori knowledge of being autoregressive with a Gaussian correlation function in clutter modeling. But Kelly's GLR and AR-GLR don't use this information so they have a poor performance as compared with AR-GC-GLR.

The AR-GC-GLR performance in comparison with AR-GLR against measured clutters is depicted in Fig. 8. An excellent performance for AR-GC-GLR detector which is the result of our suitable model and its compatibility to the real clutter conditions can be seen in this figure. As it can be seen, against a fix clutter background because of the real clutter model shape assumption, the detector has better behaviors. It is notable that in this condition the temporal correlation parameter is very close to 1.

The measured clutter is a result of several measurements on the clutter by an X band radar with the pulse duration of 300ns for 15000 samples in each experiment [14]. As it can be seen, even with no secondary data, the detector has acceptable performance especially against stationary clutters.

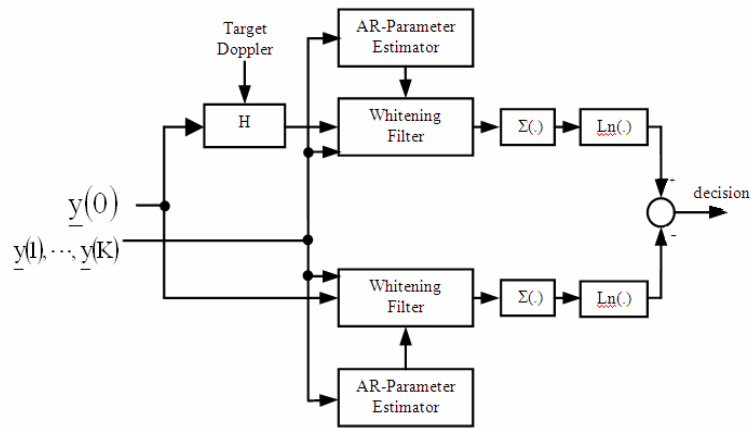


Fig. 1 Block diagram of AR-GC-GLR.

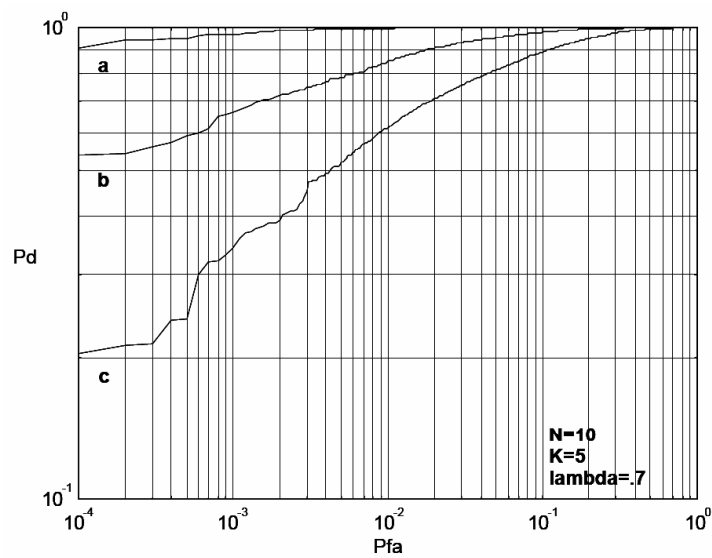


Fig. 2 Probability of detection versus probability of false alarm in various SINR conditions (a: SINR=10 dB, b: SINR=7 dB, c: SINR=5 dB).

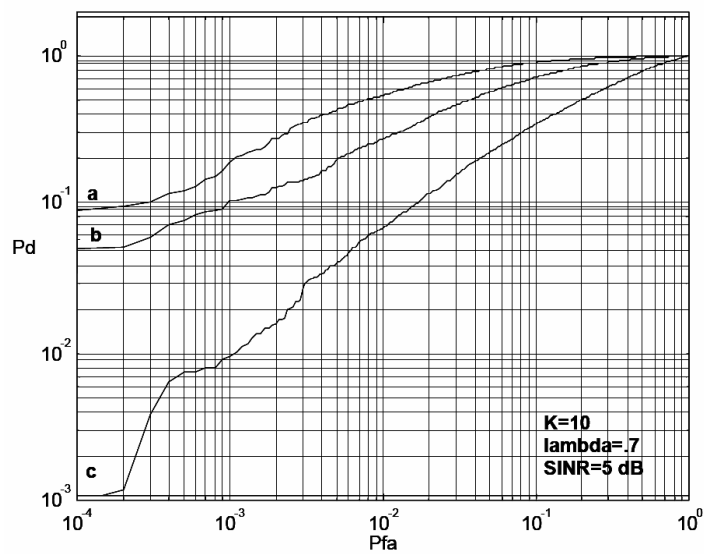


Fig. 3 Probability of detection versus probability of false alarm for three different values for the number of received radar pulses (a: N=20, b: N=10, c: N=5).

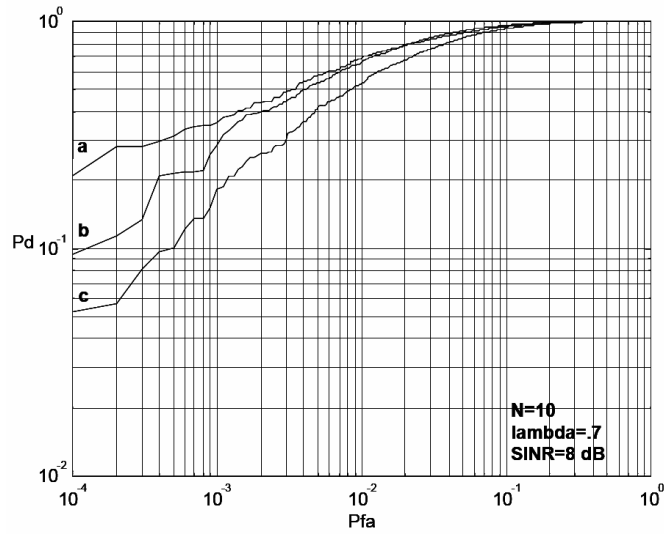


Fig. 4 Probability of detection versus probability of false alarm for three different values for the numbers of secondary data (a: $K = 20$, b: $K = 3$, c: $K = 0$).

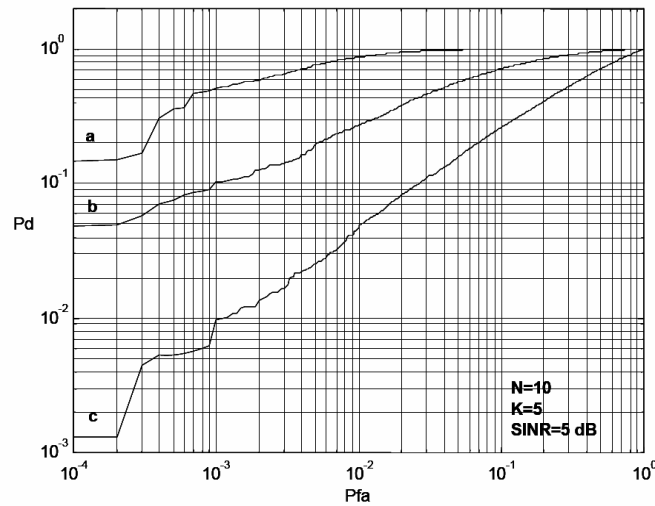


Fig. 5 Probability of detection versus probability of false alarm for various temporal correlation parameter (a: $\lambda = 0.9$, b: $\lambda = 0.7$, c: $\lambda = 0.5$).

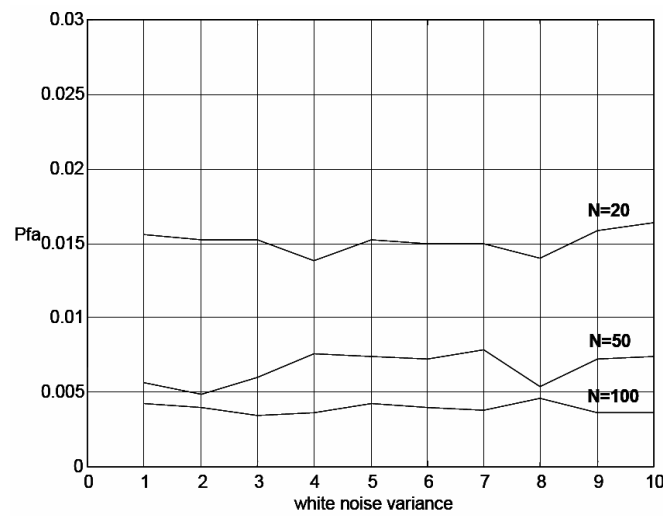
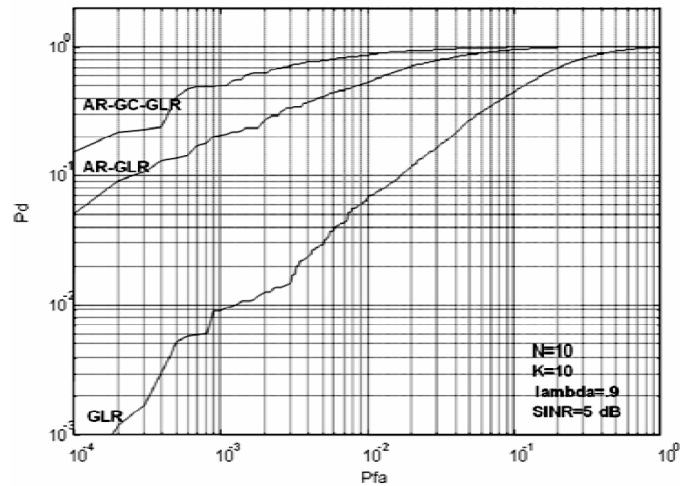
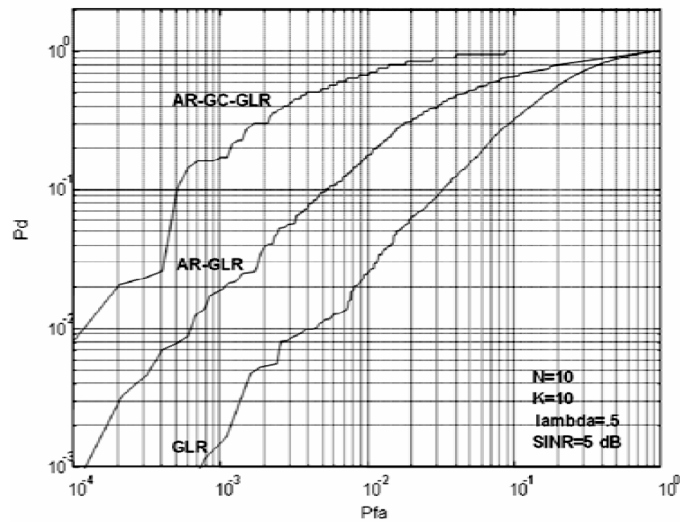


Fig. 6 P_{fa} against σ_u^2 (a: $N = 20$, b: $N = 50$, c: $N = 100$).

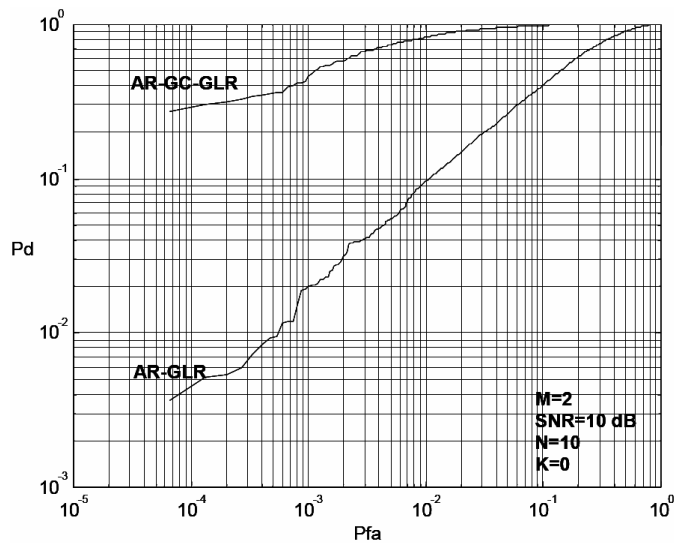


(a) $\lambda = 9$

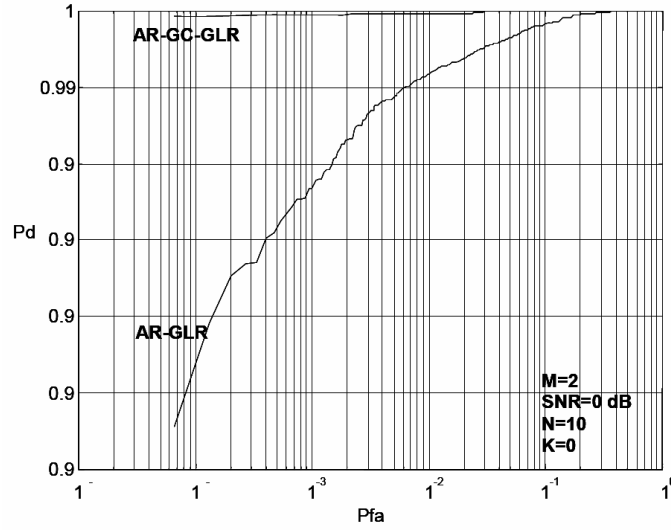


(b) $\lambda = 5$

Fig. 7 Comparison with Kelly's GLR and AR-GLR detector.



(a) Rain clutter, Range: 320 meters



(b) Ground with sparse plant coverage, Range: 2750 meters

Fig. 8 Comparison with AR-GLR against measured clutters.

5 Conclusion

In this paper, we have considered a detector for the case of a radar target with known Doppler and unknown complex amplitude in complex Gaussian noise with unknown parameters. We have applied GLR theory in this problem and we have used a model-based approach where the signal form is known and colored additive interference is characterized by AR Gaussian process with Gaussian spectrum which is a suitable model for ground clutter in most scenarios involving airborne radars. Furthermore, testing the detector behavior with computer simulated and also practically measured clutter show its superiority in comparison with Kelly's GLR and AR-GLR detectors. It has been shown that for a moderate size of data record the AR-GC-GLR is approximately CFAR with respect to AR model driving noise variance.

The AR-GC-GLR detector doesn't need to have a separate set of data vectors (secondary data) for adaptation and can estimate the statistics of the environment using only the data under test. This property is very important in non-homogeneous or rapidly varying environments such as airborne radars in which enough secondary data is not available.

Appendix

Derivation of AR-GC-GLR Detector:

Under H_0 , the joint PDF of received signals $\mathbf{y}(k)$ is given by Eq. (14) which can be written as

$$f_0 = f_Y(\mathbf{y}(0), \mathbf{y}(1), \dots, \mathbf{y}(K) | H_0, \sigma_u^2, \lambda, \alpha = 0) \\ \cong \left(\frac{1}{\pi^N \sigma_u^{2N}} \right)^{K+1} \exp \left(-\frac{1}{\sigma_u^2} (\mathbf{u} - \mathbf{Y}\mathbf{a}(\lambda))^H (\mathbf{u} - \mathbf{Y}\mathbf{a}(\lambda)) \right) \quad (25)$$

By the definition of the GLR, we should maximize f_0 over the unknown parameter λ . Maximizing Eq. (25) over λ yields to Eq. (18). Next the maximization of f_0 over the unknown parameter σ_u^2 has been solved in ([15] p. 56) and the maximum likelihood estimates of λ and σ_u^2 under H_0 are given by Eqs. (16) and (18). Using Eq. (16) in Eq. (25) yields

$$\max_{\lambda, \sigma_u^2} \{ \ln f_0 \} \cong -N(K+1) (\ln(\pi \hat{\sigma}_u^2) + 1) \quad (26)$$

where $\hat{\sigma}_u^2$ is given by (17).

Under H_1 , the joint PDF of received signals is given by Eq. (13). To obtain the maximum likelihood estimates of the unknown parameters λ , σ_u^2 and α under H_1 , we first maximize f_1 over α which is equivalent to minimize the operand of $\exp(\bullet)$, i.e.

$$A = \min_{\alpha} \left\{ \sum_{k=0}^K \sum_{n=M+1}^N \left| x_{k,n} - \sum_{j=1}^M a_j(\lambda) x_{k,n-j} \right|^2 \right\} \\ = \sum_{k=1}^K \sum_{n=M+1}^N \left| x_{k,n} - \sum_{j=1}^M a_j(\lambda) x_{k,n-j} \right|^2 \quad (27) \\ + \min_{\alpha} \left\{ \sum_{n=M+1}^N \left| x_{0,n} - \sum_{j=1}^M a_j(\lambda) x_{0,n-j} \right|^2 \right\}$$

We define:

$$\mathbf{e} = [e_{M+1} \quad \dots \quad e_N]^T \quad (28)$$

where

$$e_n = y_{0,n} - \sum_{j=1}^M a_j(\lambda) y_{0,n-j} \quad (29)$$

and

$$\underline{\psi} = [\psi_{M+1} \quad \dots \quad \psi_N]^T \quad (30)$$

where

$$\psi_n = s_n - \sum_{j=1}^M a_j(\lambda) s_{n-j} \quad (31)$$

and since $s_n = e^{j(n-1)\Omega}$, we have $\Psi_{n+1} = e^{j\Omega} \Psi_n$ and so

$$\underline{\psi} = \psi_{M+1} \begin{bmatrix} 1 & e^{j\Omega} & \dots & e^{j(N-1)\Omega} \end{bmatrix}^T = \psi_{M+1} \boldsymbol{\Phi} \quad (32)$$

where $\boldsymbol{\Phi}$ is defined in Eq. (22). Using these definitions, we have

$$\sum_{n=M+1}^N \left| x_{0,n} - \sum_{j=1}^M a_j(\lambda) x_{0,n-j} \right|^2 = |\mathbf{e} - \alpha \underline{\psi}|^2 \quad (33)$$

Now, to find the minimum value of Eq. (33) to use in Eq. (27), we first minimize Eq. (33) which can be considered as a least square problem and its solution is given by:

$$B = \min_{\alpha} \{ |\mathbf{e} - \alpha \underline{\psi}|^2 \} = |\mathbf{e}|^2 - \frac{|\mathbf{e}^H \underline{\psi}|^2}{\underline{\psi}^H \underline{\psi}} \quad (34)$$

$$\hat{\alpha}_{ML} = \frac{\underline{\psi}^H \mathbf{e}}{\underline{\psi}^H \underline{\psi}}$$

Now to maximize f_1 over $\underline{\mathbf{a}}(1)$ and s_u^2 , we rewrite Eq. (34) as:

$$B = |\mathbf{e}|^2 - \frac{|\mathbf{e}^H \underline{\psi}|^2}{\underline{\psi}^H \underline{\psi}} = \mathbf{e}^H \mathbf{H} \mathbf{e} \quad (35)$$

$$\mathbf{H} = \mathbf{I} - \frac{\underline{\psi} \underline{\psi}^H}{\underline{\psi}^H \underline{\psi}} = \mathbf{I} - \frac{\boldsymbol{\Phi} \boldsymbol{\Phi}^H}{\boldsymbol{\Phi}^H \boldsymbol{\Phi}}$$

We see that H is not a function of $\underline{\mathbf{a}}(1)$. On the other hand, $\mathbf{e} = \mathbf{u}_0 - \mathbf{Y}_0 \underline{\mathbf{a}}(1)$, so

$$B = (\mathbf{u}_0 - \mathbf{Y}_0 \underline{\mathbf{a}}(\lambda))^H \mathbf{H} (\mathbf{u}_0 - \mathbf{Y}_0 \underline{\mathbf{a}}(\lambda)) \quad (36)$$

Since H is an idempotent matrix, we have:

$$B = (\mathbf{u}_0 - \mathbf{Y}_0 \underline{\mathbf{a}}(\lambda))^H \mathbf{H} (\mathbf{u}_0 - \mathbf{Y}_0 \underline{\mathbf{a}}(\lambda)) \quad (37)$$

$$= (\underline{\mathbf{u}}'_0 - \underline{\mathbf{Y}}'_0 \underline{\mathbf{a}}(\lambda))^H (\underline{\mathbf{u}}'_0 - \underline{\mathbf{Y}}'_0 \underline{\mathbf{a}}(\lambda))$$

where $\mathbf{Y}_0 \underline{\mathbf{c}}$ and $\mathbf{u}_0 \underline{\mathbf{c}}$ are defined in Eq. (20). So, to find the maximum likelihood estimation of $\underline{\mathbf{a}}(1)$ and σ_u^2 under H_1 , we have to solve the following maximization problem:

$$\max_{\underline{\mathbf{a}}(\lambda), \sigma_u^2} \left\{ \left(\frac{1}{\pi^N \sigma_u^{2N}} \right)^{K+1} \exp \left\{ -\frac{1}{\sigma_u^2} (\underline{\mathbf{u}}'_0 - \underline{\mathbf{Y}}'_0 \underline{\mathbf{a}}(\lambda))^H \mathbf{H} (\underline{\mathbf{u}}'_0 - \underline{\mathbf{Y}}'_0 \underline{\mathbf{a}}(\lambda)) \right\} \right\}$$

where $\underline{\mathbf{Y}} \underline{\mathbf{c}}$ and $\underline{\mathbf{u}} \underline{\mathbf{c}}$ are defined in Eq. (20). This is the same problem as Eqs. (25) and (26) if we replace $\underline{\mathbf{Y}}$ by $\underline{\mathbf{Y}} \underline{\mathbf{c}}$ and $\underline{\mathbf{u}}$ by $\underline{\mathbf{u}} \underline{\mathbf{c}}$. So using the solution of Eqs. (25) and (26), we arrive at Eqs. (19) and (23) and we have:

$$\max_{\sigma_u^2, \lambda, \alpha} \{ \ln f_1 \} \cong -N(K+1) (\ln(\hat{\sigma}_u^2) + 1) \quad (38)$$

where s_u^2 is given by Eq. (19). Finally, by using Eqs. (26) and (38), we obtain the AR-GC-GLR detector given by Eq. (15).

References

- [1] Reed I. S., Mallet J. D. and Brennan L. E., "Rapid convergence rate in adaptive arrays," *IEEE Trans. AES-10*, No. 6, pp. 853-863, Nov. 1974.
- [2] Kelly E. J., "An adaptive detection algorithm," *IEEE Trans. AES-22*, No. 2, pp. 115-127, Mar. 1986.
- [3] Wang H. and Cai L., "On adaptive multiband signal detection with the SMI algorithm," *IEEE Trans. AES-26*, No. 5, pp. 768-773, Sep. 1990.
- [4] Wang H. and Cai L., "On adaptive multiband signal detection with the GLR algorithm," *IEEE Trans. AES-27*, No. 2, pp. 225-233, Mar. 1991.
- [5] Wang H. and Cai L., "Performance Comparison of Modified SMI and GLR Algorithms," *IEEE Trans. AES-27*, No. 3, pp. 487-491, May 1991.
- [6] Sheikhi A., Nayebi M. M. and Aref M. R., "Adaptive detection algorithm for radar signals in Auto-Regressive interference," *IEE proc. Radar, Sonar and Navigation*, Vol. 145, No. 5, pp. 309-314, Oct. 1998.
- [7] Kay S. M., "Asymptotically optimum detection in unknown colored noise via Autoregressive modeling," *IEEE Trans. ASSP-31*, No. 4, pp. 927-940, Aug. 1983.
- [8] Sengupta D. and Kay S. M., "Parameter Estimation and GLRT Detection in Colored Non-

- Gaussian Autoregressive Processes,” IEEE Trans. ASSP-38, No. 10, pp. 1661-1676, Oct. 1990.
- [9] Moniri M. R., Sheikhi A. and Nayebi M. M., “A multichannel Auto-Regressive GLR detector for airborne phased array radar application,” Proc. of IEEE International Conference on Radar , Hilton Adelaide, South Australia, pp. 206-211, Sep. 3-5, 2003.
- [10] Michels J. H., “Synthesis of multichannel Auto-Regressive random processes and ergodicity considerations,” RADC-TR-90-211, July, 1990.
- [11] Kay S. M., “More Accurate Auto-Regressive Parameter and Spectral Estimation for Short Data Records,” Presented at ASSP workshop on Spectral Estimation. Hamilton, Ontario, Canada, Aug. 17-18, 1981.
- [12] Nayebi M. M. and Aref M. R., “CALR and CGLR Algorithm for Detection of Radar Signals in Clutter,” Proceeding of the International Symposium on Noise and Clutter Rejection in Radars and Imaging Sensors, ISNCR-94, IEICE, Kawasaki, Japan, pp. 271-276, Nov. 15-17, 1994.
- [13] Robey F. C., Fuhrmann D. R., Kelly E. J. and Nitzberg R., “A CFAR adaptive matched filter detector,” IEEE Trans. AES-28, No. 1, pp. 208-216, Jan. 1992.
- [14] Sheikhi A., “Adaptive detection of radar targets,” Ph.D. dissertation, Sharif University of Technology, Tehran, Iran, 1998.
- [15] Haykin S. S. and Steinhardt A., “Adaptive Radar Detection and Estimation”, NY, USA: John Wiley, 1992.
- [16] Moniri M. R., Nayebi M. M. and Sheikhi A., “A GLR detector in Auto-Regressive Interference with Gaussian spectrum for airborne radar applications,” Proc. of the International Radar Symposium, IRS2004, Warszawa, Poland, pp. 227-232, May 19-21, 2004.



Mohammad-Reza Moniri was born in Tehran, IRAN in 1975. He received the B.Sc. degree in 1997 and M.Sc. in 1999 in Electronics Engineering both from Sharif University of Technology, Tehran, IRAN and Ph.D. in 2005 in Communications Engineering from Oloom-va-Tahghighat Islamic Azad University, Tehran, IRAN.

Since 2000, he has been with the Electrical and Electronics Engineering Department, Shahr-e-Rey Islamic Azad University.

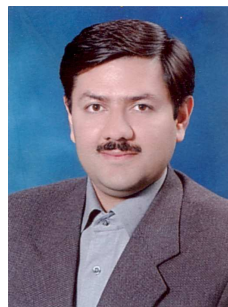
His main interests are Radar Signal Processing, Electronic Warfare and Industrial Automation.



Mohammad-Mahdi Nayebi received the B.Sc. degree in 1988 and M.Sc. in 1990 in Electronics Engineering both from Sharif University of Technology and Ph.D. in 1994 in Communications Engineering from Tarbiat Modarres University, Tehran, IRAN, all with first class honors.

Since 1991, he has been with the Electrical Engineering Department, Sharif University of Technology.

His current research interest lies in the field of Radar Signal Processing, Detection & Estimation Theory, Pattern Recognition, Electronic Warfare, Electromagnetic Compatibility and Communications.



Abbas Sheikhi was born in Shiraz, IRAN in 1971. He received the B.Sc. degree in 1993, from Shiraz University in Electronics Engineering, M.Sc. in 1995 in Biomedical Engineering and Ph.D. in 1999 in Communications Engineering both from Sharif University of Technology, Tehran, IRAN, all with first class honors.

Since 1999, he has been with the Electrical and Electronics Engineering Department, Shiraz University.

His current research interest lies in the field of Statistical Signal Processing in Radar Systems.